THE JOURNAL OF PHYSICAL CHEMISTRY C

Article

pubs.acs.org/JPCC

Energetics of Alkali and Alkaline Earth Ion-Exchanged Zeolite A

Hui Sun,[†,‡] Di Wu,[*,‡,§] Kefeng Liu,[†] Xiaofeng Guo,[‡,∥] and Alexandra Navrotsky[*,‡]

[†]State Key Laboratory of Chemical Engineering, East China University of Science and Technology, Shanghai 200237, China

[‡]Peter A. Rock Thermochemistry Laboratory and NEAT ORU, University of California, Davis, One Shields Avenue, Davis, California 95616, United States

[§]The Gene and Linda Voiland School of Chemical Engineering and Bioengineering, Washington State University, Pullman, Washington 99163, United States

[∥]Earth System Observations, Earth and Environmental Sciences Division, Los Alamos National Laboratory, Los Alamos, New Mexico 87545, United States

ABSTRACT: Alkali and alkaline earth ion-exchanged zeolite A samples were synthesized in aqueous exchange media. They were thoroughly studied by powder X-ray diffraction (XRD), electron microprobe (EMPA), thermogravimetric analysis and differential scanning calorimetry (TG-DSC), and high temperature oxide melt solution calorimetry. The hydration energetics and enthalpies of formation of these zeolite A materials from constituent oxides were determined. Specifically, the hydration level of zeolite A has a linear dependence on the average ionic potential (Z/r) of the cation, from 0.894 (Rb-A) to 1.317 per TO_2 (Mg-A). The formation enthalpies from oxides (25 °C) range from −93.71 ± 1.77 (K-A) to −48.02 ± 1.85 kJ/mol per TO_2 (Li-A) for hydrated alkali ion-exchanged zeolite A, and from −47.99 ± 1.20 (Ba-A) to −26.41 ± 1.71 kJ/mol per TO_2 (Mg-A) for hydrated alkaline earth ion-exchanged zeolite A. The formation enthalpy from oxides generally becomes less exothermic as Z/r increases, but a distinct difference in slope is observed between the alkali and the alkaline earth series.

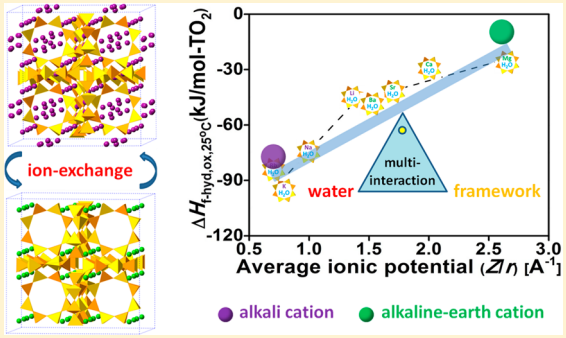

INTRODUCTION

Zeolites are microporous aluminosilicate materials with open framework structures and editable chemical properties. Their unique topologies and tunability enable applications such as molecular sieving, selective adsorption, ion exchange, heterogeneous catalysis, biomolecular engineering, and nanomedicine.[1−3] The basic building units of zeolites are corner sharing tetrahedra (TO_4, T = Si, Al). Substitution of Si^{4+} by Al^{3+} creates net negative charges ($Si^{4+} = Al^{3+} + 1/z\ M^{z+}$), which are balanced by relatively loosely held cage-residing cations. For ideal zeolite A structure, the number of SiO_4 and AlO_4 tetrahedra is equal (Si/Al = 1). This ratio leads to high hydrophilicity and large ion-exchange capacity. The accessibility (cage aperture) of zeolite A to small molecules (water and organics) can be fine-tuned by manipulating the type and content of cations.[4−10]

The ion-exchange properties of zeolite A lay the foundation for applications in the chemical industry. For instance, zeolite K-A (2.9 Å, the central or α cage aperture size) can be used for removal of water from alcohols and other gases.[4−6] Zeolite Na-A (3.8 Å) shows outstanding selectivity in propylene/propane and nitrogen/oxygen separation.[7,8] Zeolite Ca-A (4.3 Å) admits normal paraffins to its main (α) cages, yet excludes branched chain and cyclic paraffins, making it one of the most effective sorbents for *n*−*iso* paraffin separation.[9] Moreover, transition metal ion-exchanged zeolite A provides Brönsted acid sites for heterogeneous catalysis.[11−14] On the other hand, the internal void space of ion-exchanged zeolite A may host water molecules, which hydrate the cations and fill the cages. Hence, it is fundamentally vital and practically necessary to investigate the energetics of ion exchange and hydration, which directly govern the structure, phase, stability, accessibility, and functionality of zeolite A.[15,16]

The energetics of several ion-exchanged zeolites, including zeolite β, Y, and natrolite, have been investigated by direct calorimetric measurement of heats of formation.[17−21] Very recently, we studied the energetics of Na−Ca ion-exchanged zeolite A with different calcium contents using high temperature oxide melt solution calorimetry.[22] We found that the overall energetics and degree of hydration of Na−Ca ion-exchanged zeolite A are tightly correlated with the average ionic potential of guest cations (Z/r, defined as $\sum X_i(Z/r)/\sum X_i$), where X is mole fraction, Z is charge, and r is ionic radius.[22] Similar thermochemical trends have been reported for alkali and alkaline earth ion-exchanged zeolite β and Y.[17,18,20,21] However, a thorough investigation into the energetic stability and hydration of alkali and alkaline earth ion-exchanged zeolite A (Figure 1) has not been systematically carried out.

Received: May 12, 2016
Revised: June 30, 2016
Published: June 30, 2016

DOI: 10.1021/acs.jpcc.6b04840
J. Phys. Chem. C 2016, 120, 15251−15256

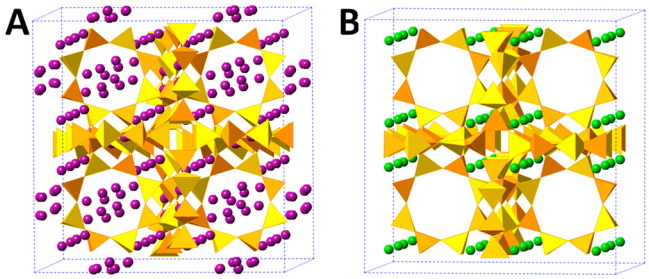

Figure 1. Framework structures of (A) alkali (Li^+, Na^+, K^+, Rb^+) and (B) alkaline earth (Mg^{2+}, Ca^{2+}, Sr^{2+}, Ba^{2+}) ion-exchanged zeolite A. Yellow tetrahedra represent AlO_4 and SiO_4, while colored spheres represent metal cations, purple for alkali and green for alkaline earth cations.

In this study, we employ high temperature oxide melt solution calorimetry as the major technique. Calorimetry, coupled with XRD, EMPA, and TG-DSC, documents the structural, chemical, and thermodynamic evolution of zeolite A upon exchange by alkali and alkaline earth cations. In light of this set of results, we identify a distinct variation in the trend of formation energetics between zeolite A with monovalent and divalent cations. We also discuss their complex, multifactor hydration phenomena, which demonstrate well-balanced site binding and nanoconfinement of water in zeolite cages.

EXPERIMENTAL METHODS

Preparation and Characterization of Ion-Exchanged Zeolite A. Synthetic zeolite Na-A (RM 8851, NIST) was used as the starting framework material. Alkali and alkaline earth metal chloride aqueous solutions (0.25 M) were prepared, serving as ion-exchange media. The detailed exchange procedure was described elsewhere.[23] For clarity, we labeled all ion-exchanged zeolite A as M-A, with M denoting the metal cations. Sample phase purity was examined by powder X-ray diffraction (XRD) employing a Bruker-AXS D8 Advance X-ray diffractometer operated at 40 kV and 40 mA using Cu Kα radiation (λ = 1.5406 Å). Data were collected in the 2θ range of 5−60° (0.02° and 1 s per step). The results were refined using Jade 6.0 and the ICSD database. Chemical compositions of all samples were characterized using a Cameca SX-100 electron microprobe (EMPA) operated at 15 kV and 10 nA. Eight testing points at different positions were randomly selected on each specimen.

A Netzsch STA 449 instrument was used for thermogravimetry and differential scanning calorimetry (TG-DSC). In each measurement, ∼20 mg of sample was hand-pressed into a pellet, placed in a Pt crucible, and heated from ambient temperature to 1200 °C (10 °C/min) under argon flow (40 mL/min). The water content of each sample was obtained from the total weight loss of its TG curve. Dehydration enthalpies of samples relative to liquid water were derived from integration of DSC peaks below 750 °C and corrected using the known enthalpy of water vaporization (44 kJ/mol of water at 25 °C).

Calorimetry. A custom-built Tian-Calvet twin calorimeter was used for high temperature oxide melt drop solution calorimetry. The methodology was described in detail elsewhere.[24,25] Fully hydrated sample pellets (∼5 mg) were dropped from ambient temperature into the calorimeter containing the solvent, molten lead borate ($2PbO{\cdot}B_2O_3$), kept at 704 °C in the calorimeter. All experiments were performed under argon flow (100 mL/min) to expel the evolved water vapor generated by dissolution of hydrated samples. The measurement was repeated at least six times on each sample to ensure reproducibility. Calibration of the calorimeter was achieved using the known heat content of corundum.

RESULTS AND DISCUSSION

Powder X-ray Diffraction (XRD). The powder XRD patterns of all samples are represented in Figure 2. Upon ion exchange, all zeolite A samples maintain LTA topology except Ba-A, which shows significant degradation of crytstallinity, as observed in previous studies.[26,27] Attempts at Ba exchange with shorter exchange period leads to similar XRD patterns. Therefore, calorimetric data on the Ba-exchanged sample are somewhat less reliable.

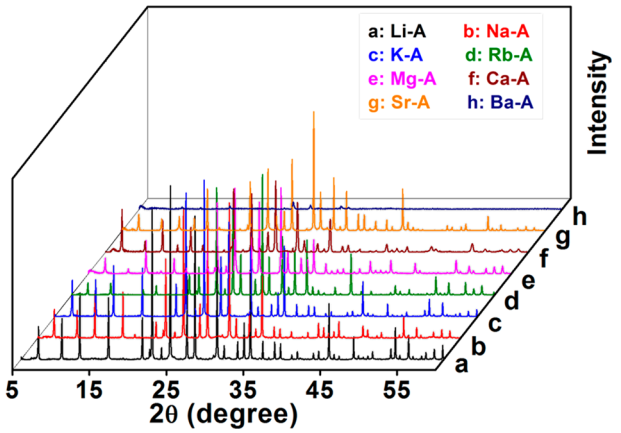

Figure 2. Powder XRD patterns of alkali and alkaline earth ion-exchanged zeolite A.

Chemical Analysis. The chemical composition and molar mass (per mole of TO_2) of all samples are summarized in Table 1. Ion exchange does not modify the Si/Al ratio of zeolite A (1.00−1.03). Na^+ is nearly fully exchanged (>97%) by Ca^{2+}, Sr^{2+}, and Ba^{2+}, while K^+ and Rb^+ replace 90% Na^+. Interestingly, Li-A has the smallest degree of exchange (76.6%), which may be due to its low ion selectivity compared with that of Na^+.[28,29]

Thermogravimetric Analysis and Differential Scanning Calorimetry (TG-DSC). Each TG curve has a major weight loss due to framework dehydration, spanning 30 to roughly 600 °C (see Figure 3A). The number of water molecules per TO_2 unit for each sample is plotted in Figure 3B. Generally, substitution of monovalent cations by divalent cations leads to site occupancy variation, which greatly modifies the hydration level of ion-exchanged zeolite A. Specifically, the degree of hydration of zeolite M-A tends to increase as the average ionic potential increases, ranging from 0.984 per TO_2 for Rb-A to 1.317 per TO_2 for Mg-A.

The DSC profiles for all samples are presented in Figure 3C. Here we mainly focused on temperatures lower than 800 °C, at which no obvious framework collapse is observed. Dehydration results in one major broad endothermic peak for each sample. This peak tends to be broader as the ionic radius increases, from Li^+ to Rb^+ or from Mg^{2+} to Ba^{2+}. Interestingly, all alkali zeolites show a single dehydration peak, whereas two well-resolved, broad endothermic signals are observed for dehydration of alkaline earth zeolites. Although similar phenomena were also seen in our previous study on

DOI: 10.1021/acs.jpcc.6b04840
J. Phys. Chem. C 2016, 120, 15251−15256

Table 1. Chemical Compositions and Lattice Parameters of Zeolite M-A on TO_2 Basis

zeolite	chemical composition	weight of H_2O (%)	H_2O per cation	MW	a (Å)
Li-A	$Li_{0.436}Na_{0.133}Al_{0.495}Si_{0.505}O_{2.037}\cdot 1.040H_2O$	22.04	2.39	84.95	24.5923(321)
Na-A[a]	$Na_{0.480}Al_{0.491}Si_{0.509}O_{1.995}\cdot 1.011H_2O$	20.52	2.11	88.70	24.6187(3)
K-A	$K_{0.453}Na_{0.037}Al_{0.492}Si_{0.508}O_{1.999}\cdot 0.858H_2O$	16.51	1.89	93.55	24.6618(386)
Rb-A	$Rb_{0.425}Na_{0.051}Al_{0.499}Si_{0.501}O_{1.988}\cdot 0.984H_2O$	15.46	2.32	114.53	24.6981(12)
Mg-A	$Mg_{0.197}Na_{0.094}Al_{0.492}Si_{0.508}O_{1.998}\cdot 1.317H_2O$	26.29	6.69	90.18	24.5172(21)
Ca-A[a]	$Ca_{0.249}Na_{0.011}Al_{0.490}Si_{0.510}O_{2.010}\cdot 1.210H_2O$	23.74	4.86	91.75	24.5606(9)
Sr-A	$Sr_{0.257}Na_{0.009}Al_{0.499}Si_{0.501}O_{2.012}\cdot 1.272H_2O$	21.73	4.95	105.37	24.6198(0)
Ba-A	$Ba_{0.262}Na_{0.009}Al_{0.501}Si_{0.499}O_{2.016}\cdot 0.815H_2O$	13.26	3.11	110.66	24.6890(616)

[a]Reference 22.

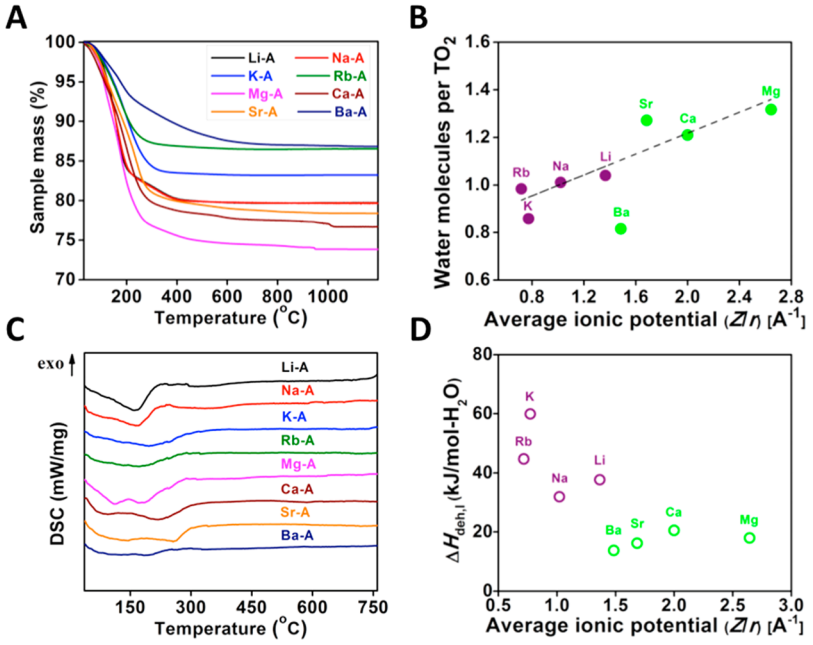

Figure 3. (A) TGA curves of hydrated alkali and alkaline earth ion-exchanged zeolite A. The data of Li-A and Na-A are nearly overlapped. (B) Water contents of hydrated alkali and alkaline earth ion-exchanged zeolite A as a function of average ionic potential. Solid points represent the measured results, while the dashed line demonstrates the linear fit. (C) DSC profiles of hydrated alkali and alkaline earth ion-exchanged zeolite A. (D) Dehydration enthalpy of hydrated alkali and alkaline earth ion-exchanged zeolite A versus average ionic potential.

dehydration of Na−Ca ion-exchanged zeolite A with different Ca contents,[22] the systematics observed here are obvious. Additionally, the dehydration enthalpies of zeolite M-A relative to liquid water ($\Delta H_{deh,l}$) were calculated by integration of DSC peaks with correction for water vaporization (Figure 3D). K-A shows the most endothermic dehydration enthalpy (59.91 ± 1.87 kJ/mol of H_2O), while Ba-A presents the least endothermic value of 13.72 ± 0.83 kJ/mol of H_2O. In general, the dehydration enthalpies of alkali zeolites tend to be more endothermic than those of alkaline earth zeolites.

Enthalpy of Formation and Hydration. The formation enthalpies of all zeolite M-A at 25 °C from constituent oxides ($\Delta H_{f\text{-}hyd,ox}$) and elements ($\Delta H_{f\text{-}hyd,el}$) were calculated from drop solution enthalpies of hydrated samples ($\Delta H_{ds\text{-}hyd}$) using the thermodynamic cycles detailed in Table 2. Table 3 lists the ΔH_{ds} values of constituent oxides. The calculated formation enthalpies of hydrated zeolite M-A samples are presented in Table 4. The general trend is that $\Delta H_{f\text{-}hyd,ox}$ becomes less exothermic linearly as the average ionic potential increases (Figure 4A). Interestingly, there appears to be a single linear trend for the alkali and for the alkaline earth zeolite M-A, with the former group exhibiting a more positive slope. For alkaline earth zeolite M-A, Mg-A has the least exothermic formation enthalpy of −26.41 ± 1.71 kJ/mol per TO_2, while Ba-A shows the most exothermic formation enthalpy of −47.99 ± 1.20 kJ/mol per TO_2. On the other hand, for alkali zeolite M-A, Li-A has the least exothermic formation enthalpy of −48.02 ± 1.85 kJ/mol per TO_2. Nevertheless, it is K-A rather than Rb-A that shows the most negative formation enthalpy (−93.71 ± 1.77 kJ/mol per TO_2), which deviates slightly from the linear trend of formation enthalpy as a function of average ionic potential.

The enthalpy of formation ($\Delta H_{f\text{-}hyd,ox}$) of hydrated zeolite A at 25 °C from constituent oxides includes two terms, $\Delta H_{hyd,l}$ ($-\Delta H_{deh,l}$) and $\Delta H_{f\text{-}deh,ox}$. $\Delta H_{hyd,l}$ is the enthalpy of hydration of the same dehydrated framework at 25 °C relative to liquid water, while $\Delta H_{f\text{-}deh,ox}$ is the formation enthalpy of the corresponding dehydrated zeolite at 25 °C from constituent oxides. In principle, $\Delta H_{f\text{-}deh,ox}$ reflects purely the structural stability of the zeolite framework. $\Delta H_{f\text{-}hyd,ox}$ and $\Delta H_{f\text{-}deh,ox}$ are plotted against the average ionic potential (Figure 4). Both of these enthalpies are exothermic with $\Delta H_{f\text{-}hyd,ox}$ being more exothermic than $\Delta H_{f\text{-}deh,ox}$ (since hydration is exothermic).

For each zeolite topology with the same Si/Al ratio, the enthalpy of formation tends to be less exothermic as Z/r increases.[16,38] Such a trend reflects the acid−base chemistry of ternary oxide formation[16,38] and is also seen in this study.

DOI: 10.1021/acs.jpcc.6b04840
J. Phys. Chem. C 2016, 120, 15251−15256

Table 2. Thermodynamic Cycles for Formation Enthalpies of Zeolite M-A from Oxides[a]

Enthalpy of Formation of Zeolite Na-A	
$x/2Na_2O$ (soln, 704 °C) + $y/2Al_2O_3$ (soln, 704 °C) + $zSiO_2$ (soln, 704 °C) + mH_2O (g, 704 °C) → $Na_xAl_ySi_zO_2{\cdot}mH_2O$ (s, 25 °C)	$\Delta H_1 = \Delta H_{ds\text{-}hyd}$
Na_2O (s, 25 °C) → Na_2O (soln, 704 °C)	ΔH_2
Al_2O_3 (s, 25 °C) → Al_2O_3 (soln, 704 °C)	ΔH_3
SiO_2 (s, 25 °C) → SiO_2 (soln, 704 °C)	ΔH_4
H_2O (l, 25 °C) → H_2O (g, 704 °C)	ΔH_5
$x/2Na_2O$ (s, 25 °C) + $y/2Al_2O_3$ (s, 25 °C) + $zSiO_2$ (s, 25 °C) + mH_2O (l, 25 °C) → $Na_xAl_ySi_zO_2{\cdot}mH_2O$ (s, 25 °C)	$\Delta H_6 = \Delta H_{f\text{-}hyd,ox}$
$\Delta H_6 = \Delta H_1 + x/2\Delta H_2 + y/2\Delta H_3 + z\Delta H_4 + m\Delta H_5$	
Enthalpy of Formation of Other Ion-Exchanged Zeolite A	
$a/2Na_2O$ (soln, 704 °C) + $bq/2M_{2/q}O$ (soln, 704 °C) + $c/2Al_2O_3$ (soln, 704 °C) + $dSiO_2$ (soln, 704 °C) + nH_2O (g, 704 °C) → $Na_aM_bAl_cSi_dO_2{\cdot}nH_2O$ (s, 25 °C) (M = Li, K, Rb, Mg, Ca, Sr, or Ba)	$\Delta H_7 = \Delta H_{ds\text{-}hyd}$
Na_2O (s, 25 °C) → Na_2O (soln, 704 °C)	ΔH_2
Al_2O_3 (s, 25 °C) → Al_2O_3 (soln, 704 °C)	ΔH_3
SiO_2 (s, 25 °C) → SiO_2 (soln, 704 °C)	ΔH_4
H_2O (l, 25 °C) → H_2O (g, 704 °C)	ΔH_5
$M_{2/q}O$ (s, 25 °C) → $M_{2/q}O$ (soln, 704 °C)	ΔH_8
$a/2Na_2O$ (s, 25 °C) + $bq/2M_{2/q}O$ + $c/2Al_2O_3$ (s, 25 °C) + $dSiO_2$ (s, 25 °C) + nH_2O (l, 25 °C) → $Na_aM_bAl_cSi_dO_2{\cdot}nH_2O$ (s, 25 °C)	$\Delta H_9 = \Delta H_{f\text{-}hyd,ox}$
$\Delta H_9 = \Delta H_7 + a/2\Delta H_2 + bq/2\Delta H_8 + c/2\Delta H_3 + d\Delta H_4 + n\Delta H_5$	

[a] ΔH_1 and ΔH_7 are the drop solution enthalpies of zeolite A; ΔH_2, ΔH_3, ΔH_4, and ΔH_8 are the drop solution enthalpies of oxides; ΔH_5 is the drop solution enthalpy of liquid water; ΔH_6 and ΔH_9 are the formation enthalpies of zeolites from oxides; $q = 1$ for alkali cation and $q = 2$ for alkaline earth cation.

Table 3. Drop Solution Enthalpies for Constituent Oxides and Water in Molten Lead Borate at 704 °C and Their Corresponding Formation Enthalpies from Elements at 25 °C

zeolite	ΔH_{ds} (kJ/mol)	$\Delta H_{f,el}$ (kJ/mol)
lithium oxide (Li_2O)	−18.28 ± 2.17[a]	−598.73 ± 2.09[h]
sodium oxide (Na_2O)	−113.10 ± 0.83[b]	−414.82 ± 0.28[h]
potassium oxide (K_2O)	−193.68 ± 1.10[b]	−363.17 ± 2.09[h]
rubidium oxide (Rb_2O)	−216.80 ± 1.90[c]	−338.90 ± 8.40[h]
magnesium oxide (MgO)	36.48 ± 0.50[d]	−601.49 ± 0.29[h]
calcium oxide (CaO)	−17.50 ± 1.20[e]	−635.09 ± 0.88[h]
strontium oxide (SrO)	−58.50 ± 2.00[f]	−590.49 ± 0.92[h]
barium oxide (BaO)	−91.50 ± 1.90[g]	−548.10 ± 2.09[h]
corundum (Al_2O_3)	107.90 ± 1.00[e]	−1675.70 ± 1.30[h]
quartz (SiO_2)	39.10 ± 0.30[e]	−910.70 ± 1.00[h]
water (H_2O)	68.90 ± 0.10[h]	−285.83 ± 0.04[h]

[a]Reference 30. [b]Reference 31. [c]Reference 32. [d]Reference 33. [e]Reference 34. [f]Reference 35. [g]Reference 36. [h]Reference 37.

The zeolite A structure (aperture size and site occupation) is significantly modified by ion exchange, which is reflected in the enthalpies of formation. Zeolite A has two types of cavities, the sodalite (β) cage, having a fixed window of 2.8 Å, and the central (α) cage with a modifiable aperture (2.9 Å for K-A, 3.8 Å for Na-A, and 4.3 Å for Ca-A).[39] On the other hand, in each zeolite A pseudo-unit-cell there are 12 sites with negative charges, which are neutralized by alkali or alkaline earth cations.[40,41] They are, for site I, centered in the six-member rings and displaced into the α cavity, site II, located near the center of the eight-member rings and close to its planes, and site III, centered in the four-member rings and displaced into the α cavity. Typically, the site selectivity of the cation is governed by the size rather than the type of cation.[27] Smaller cations, such as Li^+, Na^+, Mg^{2+}, Ca^{2+}, and Sr^{2+}, prefer site I, while site II is much more favorable to larger cations, including K^+, Rb^+, and Ba^{2+}. For monovalent cations, the site selectivity ranks in the order I > II > III. Specifically, eight cations occupy site I first, and then three sit at site II; the last one locates at site III. In contrast, for zeolite Mg, Ca, and Sr-A, site I is occupied by five cations, while the remaining cations fill site II. Interestingly, as the divalent cation with the largest diameter, three Ba^{2+} fill site II first, and the other three Ba^{2+} occupy site I.[27] The trend of formation enthalpies observed in this study reflects these microscopic variations. A distinct difference in the energetic trend (slope of formation enthalpy plots) was observed between alkali (monovalent) and the alkaline earth (divalent) ion-exchanged zeolite A. This implies that the chemical nature and crystallographic distribution of charge-compensating cations may be crucial factors governing the stability of ion-exchanged zeolites. Although they may be less obvious for high silica zeolites,[17−21] such differences are clearly obvious for zeolites with low Si/Al ratio, such as zeolite A.

Zeolite hydration reflects complex interactions among water, cation, and framework. Our study highlights the competition and interplay between cation binding and confinement on the hydration energetics. Computational studies[42,43] suggest that, upon full hydration, an ideal Na-A pseudo-unit-cell may host 20 water molecules in the central (α) cage and four in the sodalite (β) cage, while three water molecules interact with site II (Na^+) and the remaining one is coordinated at site III (Na^+). Our experimental evidence confirms their conclusion for Na-A hydration. In addition, a positive linear relationship between the number of water molecules held in zeolite A and the average ionic potential is revealed for alkali and alkaline earth ion-exchanged zeolite A (see Figure 3B). Typically, the water−cation binding is much stronger than the confinement effect on water from cages and/or cavities.[42] Additionally, cations with higher ionic potential appear to have stronger binding with water.[42] However, this is not observed in the present study. Specifically, alkali ion-exchanged samples present more exothermic hydration enthalpies than alkaline earth ion-exchanged zeolite A. This may occur because the internal volume of each zeolite A unit cell occupied by the alkali cations is much greater than that for alkaline earth ions, simply because there are twice as many of the former. This leads to less available space and relatively stronger confinement effects on water (see Figure 1). In sharp contrast to the alkali case, for alkaline earth ion-exchanged zeolite A, the total number of cations per unit cell decreases from 12 (monovalent cation) to 6 (divalent cation). The framework is rich in accessible internal void space to host more water molecules (see Figure 1B).[44] Therefore, despite higher Z/r, the increased population of weakly associated water molecules leads to weaker average water−zeolite interactions (Figure 3D). These interpretations suggest that closely balanced competition between cation binding and cage confinement determines the hydration energetics of alkali and alkaline earth ion-exchanged zeolite A. The optimized overall free energies are achieved by fine-tuned energetics and framework composition.

■ CONCLUSIONS

The energetics of formation and hydration of alkali and alkaline earth ion-exchanged zeolite A were studied employing XRD, EMPA, TG-DSC, and high temperature oxide melt solution

DOI: 10.1021/acs.jpcc.6b04840
J. Phys. Chem. C 2016, 120, 15251−15256

Table 4. Enthalpies of Drop Solution and Formation from Oxides and Elements at 25 °C of Hydrated Zeolite M-A on TO_2 Basis[a]

zeolite	$\Delta H_{ds\text{-}hyd}$[b] (kJ/mol)	$\Delta H_{f\text{-}hyd,ox}$[c] (kJ/mol)	$\Delta H_{f\text{-}hyd,el}$[d] (kJ/mol)	$\Delta H_{deh,l}$ (kJ/mol H_2O)
Li-A	154.71 ± 1.76 (6)[e]	−48.02 ± 1.85	−1483.83 ± 2.04	37.70
Na-A[f]	163.54 ± 1.15 (6)[e]	−74.50 ± 1.21	−1426.37 ± 1.48	31.95
K-A	153.34 ± 1.72 (6)[e]	−93.71 ± 1.77	−1362.80 ± 2.01	59.91
Rb-A	153.39 ± 1.81 (6)[e]	−87.96 ± 1.88	−1390.92 ± 2.70	44.69
Mg-A	165.53 ± 1.68 (6)[e]	−26.41 ± 1.71	−1553.92 ± 1.92	17.99
Ca-A[f]	155.70 ± 1.58 (6)[e]	−30.79 ± 1.64	−1536.47 ± 1.84	20.53
Sr-A	161.38 ± 1.22 (6)[e]	−42.67 ± 1.38	−1552.25 ± 1.54	16.22
Ba-A	126.27 ± 1.05 (6)[e]	−47.99 ± 1.20	−1378.35 ± 1.49	13.72

[a]The dehydration enthalpies of zeolite A relative to liquid water ($\Delta H_{deh,l}$, kJ/mol H_2O) are also listed. [b]Drop solution enthalpy of hydrated zeolites. [c]Formation enthalpy of hydrated zeolites from oxides. [d]Formation enthalpy of hydrated zeolites from elements. [e]The values in parentheses denote the number of measurements. [f]Reference 22.

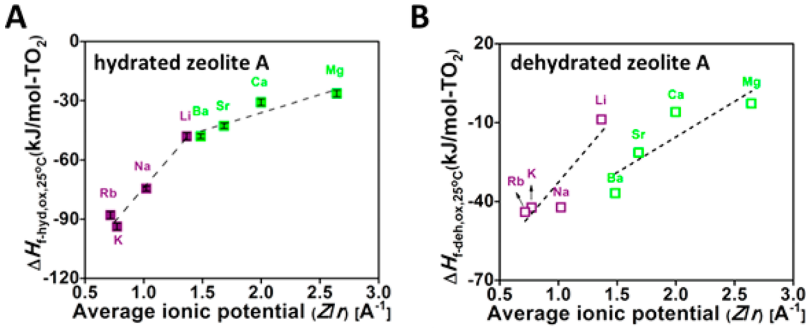

Figure 4. Enthalpy of formation of (A) hydrated and (B) dehydrated alkali and alkaline earth ion-exchanged zeolite A from oxides as a function of average ionic potential.

calorimetry. Our results suggest that all zeolite A samples investigated show increased hydration level and less exothermic enthalpies of formation as the average ionic potential of framework cation increases. Interestingly, the enthalpies of hydration of monovalent, alkali ion-exchanged zeolite A are more exothermic than those of divalent, alkaline earth ion-exchanged zeolite A. Distinct trends in plots of formation enthalpy versus ionic potential are identified for alkali and alkaline earth ion-exchanged zeolite A.

AUTHOR INFORMATION

Corresponding Authors

*E-mail: d.wu@wsu.edu. Phone: (530) 219-3497.

*E-mail: anavrotsky@ucdavis.edu. Phone: (530) 752-3292.

Notes

The authors declare no competing financial interest.

ACKNOWLEDGMENTS

This work was supported by the U.S. Department of Energy, Office of Basic Energy Sciences, Grant DE-FG02-05ER15667. H.S. thanks the Natural Science Foundation of Shanghai for the financial support (No. 16ZR1408100), and the China Scholarship Council for the State Scholarship Fund (No. 201308310077). D.W. acknowledges the institutional funds from the Gene and Linda Voiland School of Chemical Engineering and Bioengineering at Washington State University.

REFERENCES

(1) Weitkamp, J.; Puppe, L. *Catalysis and Zeolites: Fundamentals and Applications*; Springer: Heidelberg, 1999.

(2) Auerbach, S. M.; Carrado, K. A.; Dutta, P. K. *Handbook of Zeolite Science and Technology*; Taylor & Francis: London, 2003.

(3) Chen, N. Y.; Gorwood, W. E.; Dwyer, F. G. *Shape Selective Catalysis in Industrial Applications*, 2nd ed.; Macel Dekker, Inc.: New York, 1996.

(4) Carton, A.; Gonzalez, G.; De La Torre, A. I.; Cabezas, J. L. Separation of Ethanol Water Mixtures Using 3a Molecular-Sieve. *J. Chem. Technol. Biotechnol.* **1987**, *39*, 125−132.

(5) Lamberov, A. A.; Sitnikova, E. Y. Experience of the Industrial Use of Alumina and KA Zeolite in the Processes of Drying of Olefin-containing Mixtures in Petrochemical Industry. *Pet. Chem.* **2009**, *49*, 167−170.

(6) Sarkar, B.; Sunitha, K.; Sridhar, S.; Kale, V. Bioethanol Dehydration through Polyvinyl alcohol (PVA) and 3A Zeolite Mixed Matrix Composite Pervaporation Membrane. *J. Polym. Mater.* **2013**, *30*, 131−143.

(7) Grande, C. A.; Rodrigues, A. E. Propane/Propylene Separation by Pressure Swing Adsorption Using Zeolite 4A. *Ind. Eng. Chem. Res.* **2005**, *44*, 8815−8829.

(8) Yin, X. J.; Zhu, G. S.; Yang, W. S.; Li, Y. S.; Zhu, G. Q.; Xu, R.; Sun, J. Y.; Qiu, S. L.; Xu, R. R. Stainless-steel-net-supported Zeolite NaA Membrane with High Permeance and High Permselectivity for Oxygen over Nitrogen. *Adv. Mater.* **2005**, *17*, 2006−2010.

(9) Silva, J. A. C.; Da Silva, F. A.; Rodrigues, A. E. Separation of n/iso Paraffins by PSA. *Sep. Purif. Technol.* **2000**, *20*, 97−110.

(10) Sun, H.; Wu, D.; Guo, X. F.; Shen, B. X.; Liu, J. C.; Navrotsky, A. Energetics of Confinement of n-Hexane in Ca-Na Ion Exchanged Zeolite A. *J. Phys. Chem. C* **2014**, *118*, 25590−25596.

(11) Riley, P. E.; Kunz, K. B.; Seff, K. Crystal-Structure of an Ethylene Sorption Complex of Partially Cobalt(Ii)-Exchanged Zeolite A. *J. Am. Chem. Soc.* **1975**, *97*, 537−542.

(12) Campana, L.; Selloni, A.; Weber, J.; Goursot, A. Structure and Stability of Zeolite Offretite under Si4+/(Al3+,M(+)) Substitution (M = Na,K) - a First Principles Molecular-Dynamics Study. *J. Phys. Chem.* **1995**, *99*, 16351−16356.

DOI: 10.1021/acs.jpcc.6b04840
J. Phys. Chem. C 2016, 120, 15251−15256

(13) Joshi, U. D.; Joshi, P. N.; Tamhankar, S. S.; Joshi, V. P.; Idage, B. B.; Joshi, V. V.; Shiralkar, V. P. Influence of the Size of Extraframework Monovalent Cations in X-type Zeolite on Their Thermal Behavior. *Thermochim. Acta* **2002**, *387*, 121−130.
(14) Castaldi, P.; Santona, L.; Cozza, C.; Giuliano, V.; Abbruzzese, C.; Nastro, V.; Melis, P. Thermal and Spectroscopic Studies of Zeolites Exchanged with Metal Cations. *J. Mol. Struct.* **2005**, *734*, 99−105.
(15) Davis, M. E.; Lobo, R. F. Zeolite and Molecular-Sieve Synthesis. *Chem. Mater.* **1992**, *4*, 756−768.
(16) Navrotsky, A.; Trofymluk, O.; Levchenko, A. A. Thermochemistry of Microporous and Mesoporous Materials. *Chem. Rev.* **2009**, *109*, 3885−3902.
(17) Sun, P. P.; Navrotsky, A. Enthalpy of Formation and Dehydration of Alkaline Earth Cation Exchanged Zeolite Beta. *Microporous Mesoporous Mater.* **2008**, *109*, 147−155.
(18) Sun, P. P.; Deore, S.; Navrotsky, A. Formation and Dehydration Enthalpy of Ion Exchanged Zeolite Beta. *Microporous Mesoporous Mater.* **2006**, *91*, 15−22.
(19) Wu, L. L.; Navrotsky, A.; Lee, Y.; Lee, Y. Thermodynamic Study of Alkali and Alkaline-Earth Cation-exchanged Natrolites. *Microporous Mesoporous Mater.* **2013**, *167*, 221−227.
(20) Sun, P. P.; Deore, S.; Navrotsky, A. Enthalpy of Formation and Dehydration of Lithium and Sodium Zeolite Beta. *Microporous Mesoporous Mater.* **2007**, *98*, 29−40.
(21) Yang, S. Y.; Navrotsky, A. Energetics of Formation and Hydration of Ion-Exchanged Zeolite Y. *Microporous Mesoporous Mater.* **2000**, *41*, 345−346.
(22) Sun, H.; Wu, D.; Guo, X.; Shen, B.; Navrotsky, A. Energetics of Sodium-Calcium Exchanged Zeolite A. *Phys. Chem. Chem. Phys.* **2015**, *17*, 11198−11203.
(23) Sun, H.; Wu, D.; Guo, X.; Navrotsky, A. Energetics and Structural Evolution of Na-Ca Exchanged Zeolite A during Heating. *Phys. Chem. Chem. Phys.* **2015**, *17*, 9241−9247.
(24) Navrotsky, A. Progress and New Directions in High-Temperature Calorimetry. *Phys. Chem. Miner.* **1977**, *2*, 89−104.
(25) Navrotsky, A. Progress and New Directions in High Temperature Calorimetry Revisited. *Phys. Chem. Miner.* **1997**, *24*, 222−241.
(26) Sherry, H. S.; Walton, H. F. The Ion-Exchange Properties of Zeolites. II. Ion Exchange in the Synthetic Zeolite Linde 4A. *J. Phys. Chem.* **1967**, *71*, 1457−1465.
(27) Ogawa, K.; Nitta, M.; Aomura, K. Theoretical-Study of Site Selectivity of Zeolite Cation 0.1. Site Selectivities of Alkali and Alkaline-Earth Metal-Cations in Zeolite-A. *J. Phys. Chem.* **1978**, *82*, 1655−1660.
(28) Sherry, H. S. Ion-Exchange Properties of Zeolites.I. Univalent Ion Exchange in Synthetic Faujasite. *J. Phys. Chem.* **1966**, *70*, 1158−1168.
(29) Yang, S. Y.; Navrotsky, A. Energetics of Formation and Hydration of Ion-Exchanged Zeolite Y. *Microporous Mesoporous Mater.* **2000**, *37*, 175−186.
(30) Xu, H. W.; Heaney, P. J.; Navrotsky, A.; Topor, L.; Liu, J. Thermochemistry of Stuffed Quartz-derivative Phases along the Join LiAlSiO4-SiO2. *Am. Mineral.* **1999**, *84*, 1360−1369.
(31) Kiseleva, I.; Navrotsky, A.; Belitsky, I. A.; Fursenko, B. A. Thermochemistry of Natural Potassium Sodium Calcium Leonhardite and its Cation-Exchanged Forms. *Am. Mineral.* **1996**, *81*, 668−675.
(32) Xu, H. W.; Navrotsky, A.; Nyman, M.; Nenoff, T. M. Thermochemistry of Framework Titanosilicate A(2)TiSi(6)O(15) (A = K, Rb, Cs). *J. Am. Ceram. Soc.* **2005**, *88*, 1819−1825.
(33) Smelik, E. A.; Jenkins, D. M.; Navrotsky, A. A Calorimetric Study of Synthetic Amphiboles Along the Tremolite-Tschermakite Join and the Heats of Formation of Magnesiohornblende and Tschermakite. *Am. Mineral.* **1994**, *79*, 1110−1122.
(34) Kiseleva, I.; Navrotsky, A.; Belitsky, I. A.; Fursenko, B. A. Thermochemistry and Phase Equilibria in Calcium Zeolites. *Am. Mineral.* **1996**, *81*, 658−667.
(35) Bularzik, J.; Navrotsky, A.; Dicarlo, J.; Bringley, J.; Scott, B.; Trail, S. Energetics of La2-Xsrxcuo4-Y Solid-Solutions (0.0-Less-Than-or-Equal-to-X-Less-Than-or-Equal-to-1.0). *J. Solid State Chem.* **1991**, *93*, 418−429.
(36) Zhou, Z. G.; Navrotsky, A. Thermochemistry of the Y2o3-Bao-Cu-O System. *J. Mater. Res.* **1992**, *7*, 2920−2935.
(37) Robie, R. A.; Hemingway, B. S. Thermodynamic Properties of Minerals and Related Substances at 298.15 K and 1 Bar (10^5 Pascals) Pressure and at Higher Temperatures. *Geol. Surv. Bull.* **1995**, 2131.
(38) Navrotsky, A.; Tian, Z. R. Systematics in the Enthalpies of Formation of Anhydrous Aluminosilicate Zeolites, Glasses, and Dense Phases. *Chem. - Eur. J.* **2001**, *7*, 769−774.
(39) Yang, R. T. *Adsorbents: Fundamentals and Applications*; John Wiley & Sons, Inc.: New York, 2003.
(40) Breck, D. W.; Eversole, W. G.; Milton, R. M.; Reed, T. B.; Thomas, T. L. Crystalline Zeolites 0.1. The Properties of a New Synthetic Zeolite, Type-A. *J. Am. Chem. Soc.* **1956**, *78*, 5963−5971.
(41) Reed, T. B.; Breck, D. W. Crystalline Zeolites 0.2. Crystal Structure of Synthetic Zeolite, Type-A. *J. Am. Chem. Soc.* **1956**, *78*, 5972−5977.
(42) Koh, K. O.; Mu Shik, J. Theoretical Study of Ionic Selectivities and Adsorption of Water in Zeolite-A. *Zeolites* **1985**, *5*, 313−316.
(43) No, K. T.; Mu Shik Jhon, M. S. Theoretical Study of Hydration of Zeolite NaA. *J. Korean Chem. Soc.* **1979**, *23*, 11.
(44) Ogawa, K.; Nitta, M.; Aomura, K. Theoretical-Study of the Site Selectivity of the Zeolite Cation 0.2. Site Selectivities of Alkaline-Earth Metal-Cations in Dehydrated Fully Ion-Exchanged Zeolite-A. *J. Phys. Chem.* **1979**, *83*, 1235−1236.

DOI: 10.1021/acs.jpcc.6b04840
J. Phys. Chem. C 2016, 120, 15251−15256